

Noname manuscript No. (will be inserted by the editor)
---

---

# A novel lattice Boltzmann model for fourth order nonlinear partial differential equations

Zhonghua Qiao · Xuguang Yang · Yuze Zhang

Received: date / Accepted: date

**Abstract** In this paper, a novel lattice Boltzmann (LB) equation model is proposed to solve the fourth order nonlinear partial differential equation (NPDE). Different from existing LB models, a source distribution function is introduced to remove some unwanted terms in the nonlinear part of the equation. Hereby, the equilibrium distribution function is designed to follow the rule of Chapman-Enskog (C-E) analysis. Through the C-E procedure, the fourth order NPDE can be recovered perfectly from the proposed LB model. A series of numerical experiments have been carried out to solve some widely studied fourth order NPDEs, including the Kuramoto-Sivashinsky equation, Cahn-Hilliard equation with double-well potential and a fourth order diffuse interface model with Peng-Robinson equation of state. Numerical results show that the performance of the present LB model is much better than other existing LB models.

**Keywords** lattice Boltzmann method · fourth order nonlinear partial differential equation · Cahn-Hilliard equation

## 1 Introduction

In recent years, lattice Boltzmann method (LBM), which is originated from lattice gas automata (LGA) and also could be derived from the kinetic Boltzmann equa-

---

Zhonghua Qiao  
Department of Applied Mathematics, The Hong Kong Polytechnic University, Hung Hom, Hong Kong.  
E-mail: zhonghua.qiao@polyu.edu.hk

Xuguang Yang  
Corresponding author.  
School of Mathematics and Computational Science, Hunan First Normal University, Changsha, China.  
E-mail: ysfxuguang@hnfnu.edu.cn

Yuze Zhang  
Beijing International Center for Mathematical Research, Peking University, Beijing 100871, China.  
E-mail: 1906391168@pku.edu.cn

tion, has emerged as an alternative powerful method to simulate complex fluid dynamics problems and nonlinear systems [6,12,16]. In contrast to the classical computational fluid dynamics (CFD) techniques, which are developed from the discretizations of macroscopic continuum equations, LBM can be regarded as a numerical method based on mesoscopic theory that connect the microscopic and macroscopic descriptions of the dynamics. The kinetic nature brings many advantages to LBM, including clear physical pictures, simple algorithm structures, easy implementation of boundary conditions and natural parallelism. Due to these attractive features, LBM has achieved great success in simulating formidable problems, such as porous media flow [10,31], multi-phase and multi-component flow [13,36,26,29], particle suspensions [22,23]. In addition, LBM has been successfully extended to solve linear and nonlinear partial differential equations (PDEs), including nonlinear isotropic and anisotropic convection-diffusion equations [7,38], wave equation [43], Burgers equation [46], Fisher equation [39] and Korteweg-de Vries (KdV) equation [9,42], etc.

From the above, we can see that LBM has become an effective numerical solver for complex nonlinear systems. However, existing works mainly focus on the second- or third-order PDEs. It is necessary to develop LBM for fourth order PDEs (such as Cahn-Hilliard equation) or more higher order PDEs. It is well known that the phase-field method, as one of interface capturing approaches, has received much attention by many researchers and has been successfully applied in the simulation of multiphase flow problems[2,18,37]. In this method, the phase interface is regarded as a transitional region with nonzero thickness, where fluid properties vary smoothly across the interface. The interface curvature and interfacial dynamics can be resolved with higher accuracy. A phase-field variable or so-called order parameter governed by the fourth order Cahn-Hilliard equation (CHE) [4,47] or the second order Allen-Cahn equation (ACE) [1] is introduced to identify different phases. Based on the fact that the CHE can conserve the mass of multiphase system, while the ACE cannot, most of works based on LBM mainly focused on the CHE [28,30,40,41,44,49,50]. [It is worth mentioning that conserved formulations based on ACE exist, see e.g., \[5\], based on which several recent LB schemes for conservative ACE have been proposed, starting with work in \[15\].](#) However, existing LBMs for CHE only treat the chemical potential as a scalar, and put it in the equilibrium distribution function. It means that existing LBMs treat CHE as a second order convection diffusion equation other than a fourth order equation. Although there are several works on fourth order PDEs [11,24,25,45], such as Kuramoto-Sivashinsky equation (KSE), the Benjamin-Ono equation, existing LB models are problem-dependent, which means that for different NPDEs, one needs to construct different LB models, including different equilibrium distribution functions and different amending functions. Recently, Chai and Shi et al. [8] proposed a general LB model for a class of NPDEs with the order up to six. To recover high-order NPDEs from their LB model, some auxiliary moments were also introduced to give the correct moments of equilibrium distribution function. But unfortunately, the fourth order NPDE, where the second order term is nonlinear (such as CHE), cannot be recovered correctly by their LB model.

In this work, we propose a general LB model for fourth order NPDEs. Different from the LB model proposed by Chai et al. [8], the fourth order NPDE with nonlinear second order term can also be solved by our LB model. Especially for solving the CHE, the chemical potential is expanded strictly following the rule of

C-E expansion, so that the present model is more precise than existing LB models. The rest of the paper is organized as follows. In section 2, a novel LBM for general fourth order nonlinear PDEs is proposed and the C-E analysis is given. In section 3, the equilibrium distribution function is defined. To validate the performance of the proposed LBM, several numerical experiments are carried out in section 4 for some widely studied fourth order NPDEs. The paper ends with some conclusions in section 5.

## 2 Lattice Boltzmann model for the fourth order NPDE

In this work, the following one dimensional (1D) fourth order NPDE is considered,

$$\partial_t \phi + \alpha_1 \partial_x \Pi_1(\phi) + \alpha_2 \partial_x^2 \Pi_2(\phi) + \alpha_3 \partial_x^3 \Pi_3(\phi) + \alpha_4 \partial_x^4 \Pi_4(\phi) = 0, \quad (1)$$

where  $\phi$  is a scalar function of position  $x$  and time  $t$ ,  $\alpha_k$  are constant coefficients, and  $\Pi_k(\phi)$  are given functions of  $\phi$ ,  $1 \leq k \leq 4$ .

### 2.1 A novel lattice Boltzmann BGK model

Our LB model is based on the D1Q $b$  lattice with  $b$  velocity directions in 1D space, given by

$$f_j(x + c_j \delta t, t + \delta t) = f_j(x, t) - \frac{1}{\tau} [f_j(x, t) - f_j^{eq}(x, t)] + \delta t F_j, \quad (2)$$

where  $\{c_j = ce_j, j = 0, \dots, b-1\}$  is the set of discrete velocity directions,  $c$  is the particle speed,  $\delta x$  and  $\delta t$  are lattice spacing and time step, respectively.  $f_j^{eq}(x, t)$  is the equilibrium distribution function (EDF), and  $F_j$  is the auxiliary source distribution function.

To solve Eq. (1),  $f_j^{eq}(x, t)$  is required to satisfy the following constrains

$$\begin{aligned} \sum_j f_j &= \sum_j f_j^{eq} = \phi, \quad \sum_j c_j f_j^{eq} = \alpha_1 \Pi_1, \\ \sum_j c_j^k f_j^{eq} &= \Pi_{k0} + \beta_k \Pi_k, \quad k = 2, \dots, m. \end{aligned} \quad (3)$$

In this work,  $m = 4$ ,  $\beta_k$  are parameters, and  $\Pi_{k0}$  are auxiliary moment (AM) functions for correctly recovering Eq. (1), which are defined as follows,

$$\Pi_{20} = \int \partial_\phi \alpha_1 \Pi_1 \partial_\phi \alpha_1 \Pi_1 d\phi, \quad (4)$$

$$\Pi_{30} = \int \partial_\phi (\Pi_{20} + 3\beta_2 \Pi_2) \partial_\phi \alpha_1 \Pi_1 d\phi = \int [(\partial_\phi \alpha_1 \Pi_1)^3 + 3\beta_2 \partial_\phi \Pi_2 \partial_\phi \alpha_1 \Pi_1] d\phi, \quad (5)$$

$$\Pi_{40} = \int \partial_\phi (2\Pi_{30} - \tilde{\Pi}_{30} + 4\beta_3 \Pi_3) \partial_\phi \alpha_1 \Pi_1 d\phi, \quad (6)$$

where  $\tilde{\Pi}_{30} = \int \partial_\phi \Pi_{20} \partial_\phi \alpha_1 \Pi_1 d\phi$ .

The auxiliary source term  $F_j$  is used to remove additional terms in the recovered macroscopic equation, which is defined as

$$F_j = \omega_j \chi \partial_x^2 (\partial_\phi \Pi_2 \partial_x^2 \phi), \quad (7)$$

where  $\omega_j = 1/b$ ,  $j = 0, \dots, b-1$ ,  $\chi = -\alpha_2(3\tau_3 - \tau_2^2)\beta_2 \delta t^2$ ,  $\tau_2 = -\tau + 1/2$ , and  $\tau_3 = \tau^2 - \tau + 1/6$ .

In addition,  $F_j$  satisfies the following moment condition

$$\sum_j F_j = \chi \partial_x^2 (\partial_\phi \Pi_2 \partial_x^2 \phi). \quad (8)$$

## 2.2 Multi-scale Chapman-Enskog analysis for the fourth order NPDE

To derive the macroscopic equation (1), the C-E expansion in time and space is applied:

$$\begin{aligned} f_j &= f_j^{(0)} + \varepsilon f_j^{(1)} + \varepsilon^2 f_j^{(2)} + \varepsilon^3 f_j^{(3)} + \varepsilon^4 f_j^{(4)}, \\ \partial_t &= \varepsilon \partial_{t_1} + \varepsilon^2 \partial_{t_2} + \varepsilon^3 \partial_{t_3} + \varepsilon^4 \partial_{t_4}, \partial_x = \varepsilon \partial_{x_1}, \end{aligned} \quad (9)$$

where  $\varepsilon$  is a small expansion parameter. Using the first equation in (3) and the relationship of  $f_j^{(0)} = f_j^{(eq)}$ , we have

$$\sum_j f_j^{(k)} = 0, 1 \leq k \leq 4. \quad (10)$$

By applying Taylor expansion to (2) to the fourth order, we get

$$D_j f_j + \frac{\delta t}{2} D_j^2 f_j + \frac{\delta t^2}{6} D_j^3 f_j + \frac{\delta t^3}{24} D_j^4 f_j + o(\delta t^3) = -\frac{1}{\tau \delta t} (f_j - f_j^{eq}) + F_j, \quad (11)$$

where  $D_j = \partial_t + c_j \partial_x$ . Substituting (9) into (11) and treating the terms in order of  $\varepsilon^k$  ( $1 \leq k \leq 4$ ) separately gives

$$O(\varepsilon^0) : f_j^{(0)} = f_j^{eq}, \quad (12)$$

$$O(\varepsilon^1) : D_{1j} f_j^{(0)} = -\frac{1}{\tau \delta t} f_j^{(1)}, \quad (13)$$

$$O(\varepsilon^2) : \partial_{t_2} f_j^{(0)} + \tau_2 \delta t D_{1j}^2 f_j^{(0)} = -\frac{1}{\tau \delta t} f_j^{(2)}, \quad (14)$$

$$O(\varepsilon^3) : \partial_{t_3} f_j^{(0)} + 2\tau_2 \delta t \partial_{t_2} D_{1j} f_j^{(0)} + \tau_3 \delta t^2 D_{1j}^3 f_j^{(0)} = -\frac{1}{\tau \delta t} f_j^{(3)}, \quad (15)$$

$$\begin{aligned} O(\varepsilon^4) : \partial_{t_4} f_j^{(0)} + 2\tau_2 \delta t \partial_{t_3} D_{1j} f_j^{(0)} + 3\tau_3 \delta t^2 \partial_{t_2} D_{1j}^2 f_j^{(0)} + \tau_2 \delta t \partial_{t_2}^2 f_j^{(0)} \\ + \tau_4 \delta t^3 D_{1j}^4 f_j^{(0)} = -\frac{1}{\tau \delta t} f_j^{(4)} + F_j^{(4)}, \end{aligned} \quad (16)$$

where  $D_{1j} = \partial_{t_1} + c_j \partial_{x_1}$ ,  $F_j^{(4)} = \omega_j \chi \partial_{x_1}^2 (\partial_\phi \Pi_2 \partial_{x_1}^2 \phi)$ , and  $\tau_4 = -\tau^3 + 3\tau^2/2 - 7/12\tau + 1/24$ .

Summing (13), (14), (15) and (16) over  $j$ , and using (3), (8) and (10), we obtain

$$\sum_j D_{1j} f_j^{(0)} = \partial_{t_1} \phi + \partial_{x_1} \alpha_1 \Pi_1(\phi) = 0, \quad (17)$$

$$\partial_{t_2} \phi + \tau_2 \delta t \sum_j D_{1j}^2 f_j^{(0)} = 0, \quad (18)$$

$$\partial_{t_3} \phi + \tau_3 \delta t^2 \sum_j D_{1j}^3 f_j^{(0)} = 0, \quad (19)$$

$$\partial_{t_4} \phi + 3\tau_3 \delta t^2 \partial_{t_2} \sum_j D_{1j}^2 f_j^{(0)} + \tau_2 \delta t \partial_{t_2}^2 \phi + \tau_4 \delta t^3 \sum_j D_{1j}^4 f_j^{(0)} = \sum_j F_j. \quad (20)$$

By using (3), (8) and (17), we have

$$\begin{aligned} \sum_j D_{1j}^2 f_j^{(0)} &= \partial_{t_1}^2 \phi + 2\partial_{t_1} \partial_{x_1} \alpha_1 \Pi_1 + \partial_{x_1}^2 (\Pi_{20} + \beta_2 \Pi_2) \\ &= \partial_{x_1} (\partial_{t_1} \alpha_1 \Pi_1 + \partial_{x_1} \Pi_{20}) + \beta_2 \partial_{x_1}^2 \Pi_2. \end{aligned} \quad (21)$$

By using (4), the following equation can be derived

$$\partial_{t_1} \alpha_1 \Pi_1 + \partial_{x_1} \Pi_{20} = \partial_\phi \alpha_1 \Pi_1 (\partial_{t_1} \phi + \partial_{x_1} \alpha_1 \Pi_1) = 0. \quad (22)$$

Then (18) can be reformulated as

$$\partial_{t_2} \phi + \alpha_2 \partial_{x_1}^2 \Pi_2 = 0, \quad (23)$$

where  $\alpha_2 = \delta t \tau_2 \beta_2$ .

Using (17) and (22), the term of  $\sum_j D_{1j}^3 f_j^{(0)}$  can be expressed as

$$\begin{aligned} \sum_j D_{1j}^3 f_j^{(0)} &= \partial_{t_1}^3 \phi + 3\partial_{t_1}^2 \partial_{x_1} \alpha_1 \Pi_1 + 3\partial_{t_1} \partial_{x_1}^2 (\Pi_{20} + \beta_2 \Pi_2) + \partial_{x_1}^3 (\Pi_{30} + \beta_3 \Pi_3) \\ &= 2\partial_{t_1}^2 \partial_{x_1} \alpha_1 \Pi_1 + 3\partial_{t_1} \partial_{x_1}^2 (\Pi_{20} + \beta_2 \Pi_2) + \partial_{x_1}^3 (\Pi_{30} + \beta_3 \Pi_3) \\ &= \partial_{x_1}^2 (\partial_{t_1} (\Pi_{20} + 3\beta_2 \Pi_2) + \partial_{x_1} \Pi_{30}) + \beta_3 \partial_{x_1}^3 \Pi_3. \end{aligned} \quad (24)$$

From (5), (19) and (24), we have

$$\partial_{t_3} \phi + \alpha_3 \partial_{x_1}^3 \Pi_3 = 0, \quad (25)$$

where  $\alpha_3 = \delta t^2 \tau_3 \beta_3$ .

Similarly, using (17), (22), (21) and (24), we obtain

$$\begin{aligned}
\sum_j D_{1j}^4 f^{(0)} &= \partial_{t_1}^4 \phi + 4\partial_{t_1}^3 \partial_{x_1} \alpha_1 \Pi_1 + 6\partial_{t_1}^2 \partial_{x_1}^2 (\Pi_{20} + \beta_2 \Pi_2) \\
&\quad + 4\partial_{t_1} \partial_{x_1}^3 (\Pi_{30} + \beta_3 \Pi_3) + \partial_{x_1}^4 (\Pi_{40} + \beta_4 \Pi_4) \\
&= 3\partial_{t_1}^3 \partial_{x_1} \alpha_1 \Pi_1 + 6\partial_{t_1}^2 \partial_{x_1}^2 (\Pi_{20} + \beta_2 \Pi_2) \\
&\quad + 4\partial_{t_1} \partial_{x_1}^3 (\Pi_{30} + \beta_3 \Pi_3) + \partial_{x_1}^4 (\Pi_{40} + \beta_4 \Pi_4) \\
&= \partial_{t_1}^2 \partial_{x_1}^2 (3\Pi_{20} + 6\beta_2 \Pi_2) + 4\partial_{t_1} \partial_{x_1}^3 (\Pi_{30} + \beta_3 \Pi_3) + \partial_{x_1}^4 (\Pi_{40} + \beta_4 \Pi_4) \\
&= \partial_{t_1}^2 \partial_{x_1}^2 \Pi_{20} + \partial_{t_1} \partial_{x_1}^3 (2\Pi_{30} + 4\beta_3 \Pi_3) + \partial_{x_1}^4 (\Pi_{40} + \beta_4 \Pi_4).
\end{aligned} \tag{26}$$

Noticing that  $\tilde{\Pi}_{30}$  satisfies  $\partial_{t_1} \Pi_{20} + \partial_{x_1} \tilde{\Pi}_{30} = 0$ , we get

$$\sum_j D_{1j}^4 f^{(0)} = \partial_{x_1}^3 (\partial_{t_1} (2\Pi_{30} - \tilde{\Pi}_{30} + 4\beta_3 \Pi_3) + \partial_{x_1} \Pi_{40}) + \beta_4 \partial_{x_1}^4 \Pi_4. \tag{27}$$

Then substituting (8) and (21) into (20), we can get the following equation

$$\partial_{t_4} \phi + 3\tau_3 \beta_2 \delta t^2 \partial_{t_2} \partial_{x_1}^2 (\Pi_2) + \tau_2 \delta t \partial_{t_2}^2 \phi + \tau_4 \beta_4 \delta t^3 \partial_{x_1}^4 (\Pi_4) = \chi \partial_{x_1}^2 (\partial_\phi \Pi_2 \partial_{x_1}^2 \phi). \tag{28}$$

From (23), we have

$$\begin{aligned}
3\tau_3 \delta t^2 \partial_{t_2} \partial_{x_1}^2 (\beta_2 \Pi_2) + \tau_2 \delta t \partial_{t_2}^2 \phi &= (3\tau_3 - \tau_2^2) \beta_2 \delta t^2 \partial_{x_1}^2 (\partial_{t_2} \Pi_2) \\
&= \chi \partial_{x_1}^2 (\partial_\phi \Pi_2 \partial_{x_1}^2 \phi).
\end{aligned} \tag{29}$$

Thus, (28) can be simplified as

$$\partial_{t_4} \phi + \tau_4 \beta_4 \delta t^3 \partial_{x_1}^4 (\Pi_4) = 0. \tag{30}$$

Combining (17), (23), (25) and (30) at different orders of  $\varepsilon$ , the general fourth order NPDE can be exactly recovered to order  $O(\varepsilon^4)$

$$\partial_t \phi + \alpha_1 \partial_x \Pi_1(\phi) + \alpha_2 \partial_x^2 \Pi_2(\phi) + \alpha_3 \partial_x^3 \Pi_3(\phi) + \alpha_4 \partial_x^4 \Pi_4(\phi) = 0, \tag{31}$$

where we enforce  $\alpha_2 = \delta t \tau_2 \beta_2$ ,  $\alpha_3 = \delta t^2 \tau_3 \beta_3$ ,  $\alpha_4 = \delta t^3 \tau_4 \beta_4$ .

*Remark 1* In previous work, the fourth order NPDE is usually numerically solved as the second order convection diffusion equation. Such as in existing LB models for CHE [28, 30, 44, 49, 50], the chemical potential  $\mu = (f'(\phi) - \kappa \phi_{xx})_{xx}$  is treated as a scalar putting in the equilibrium distribution function. Then, the scale order of the equilibrium distribution function is not  $O(\varepsilon^0)$  any more. Although Chai and Shi [8] proposed a LB model for high-order NPDEs up to order six, their model for the fourth order NPDE (1) can only solve the case of  $\Pi_2(\phi) = \phi$ . While in the present LB model,  $\Pi_2(\phi)$  is a general function of  $\phi$ , and the equilibrium distribution function is designed strictly following the rule of multi-scale C-E expansion.

*Remark 2* If we consider the fourth order NPDE with source term  $f(\phi)$ , a time-splitting scheme studied in [17] can be used. Then, the fourth order NPDE with a source term is decomposed into two subproblems,

$$\partial_t \phi = f(\phi), \tag{32}$$

$$\partial_t \phi + \alpha_1 \partial_x \Pi_1(\phi) + \alpha_2 \partial_x^2 \Pi_2(\phi) + \alpha_3 \partial_x^3 \Pi_3(\phi) + \alpha_4 \partial_x^4 \Pi_4(\phi) = 0. \tag{33}$$

### 3 The definition of equilibrium distribution function

For a given NPDE of order  $m$ , the number of discrete velocity directions is at least equal to  $m + 1$ . Thus, we can use a D1Q5 LBGK model to solve the NPDE of order less than or equal to 4.

#### 3.1 Equilibrium Distribution Functions for LBGK Model with D1Q5 lattice

Denoting  $\bar{\Pi}_0 = \phi$ ,  $\bar{\Pi}_1 = \alpha_1 \Pi_1 / c$ ,  $\bar{\Pi}_k = (\Pi_{k0} + \beta_k \Pi_k) / c^k$ ,  $k = 2, 3, 4$ , the moments conditions (3) are rewritten as

$$\sum_j e_j^k f_j^{eq} = \bar{\Pi}_k, k = 0, \dots, 4, \quad (34)$$

where  $\{e_0, e_1, e_2, e_3, e_4\} = \{0, 1, -1, 2, -2\}$ . Let

$$\vec{\Pi} = [\bar{\Pi}_0, \bar{\Pi}_1, \dots, \bar{\Pi}_4]^T, \vec{f}^{eq} = [f_0^{eq}, f_1^{eq}, \dots, f_4^{eq}]^T. \quad (35)$$

Form Eq. (34), we have

$$\mathbf{M}_5 \vec{f}^{eq} = \vec{\Pi}, \quad (36)$$

where

$$\mathbf{M}_5 = \begin{bmatrix} 1 & 1 & 1 & 1 & 1 \\ 0 & 1 & -1 & 2 & -2 \\ 0 & 1 & 1 & 4 & 4 \\ 0 & 1 & -1 & 8 & -8 \\ 0 & 1 & 1 & 16 & 16 \end{bmatrix}, \quad (37)$$

It is easy to find the inverse of  $\mathbf{M}_5$

$$\mathbf{M}_5^{-1} = \frac{1}{24} \begin{bmatrix} 24 & 0 & -30 & 0 & 6 \\ 0 & 16 & 16 & -4 & -4 \\ 0 & -16 & 16 & 4 & -4 \\ 0 & -2 & -1 & 2 & 1 \\ 0 & 2 & -1 & -2 & 1 \end{bmatrix}, \quad (38)$$

thus

$$\vec{f}^{eq} = \mathbf{M}_5^{-1} \vec{\Pi}. \quad (39)$$

Therefore, the EDFs of the LBGK model with D1Q5 lattice can be obtained as follows

$$\begin{aligned} f_0^{eq} &= [4\phi - 5\bar{\Pi}_2 + \bar{\Pi}_4]/4, \\ f_1^{eq} &= [4(\bar{\Pi}_1 + \bar{\Pi}_2) - \bar{\Pi}_3 - \bar{\Pi}_4]/6, \\ f_2^{eq} &= [4(-\bar{\Pi}_1 + \bar{\Pi}_2) + \bar{\Pi}_3 - \bar{\Pi}_4]/6, \\ f_3^{eq} &= [-2(\bar{\Pi}_1 - \bar{\Pi}_3) - \bar{\Pi}_2 + \bar{\Pi}_4]/24, \\ f_4^{eq} &= [2(\bar{\Pi}_1 - \bar{\Pi}_3) - \bar{\Pi}_2 + \bar{\Pi}_4]/24. \end{aligned}$$

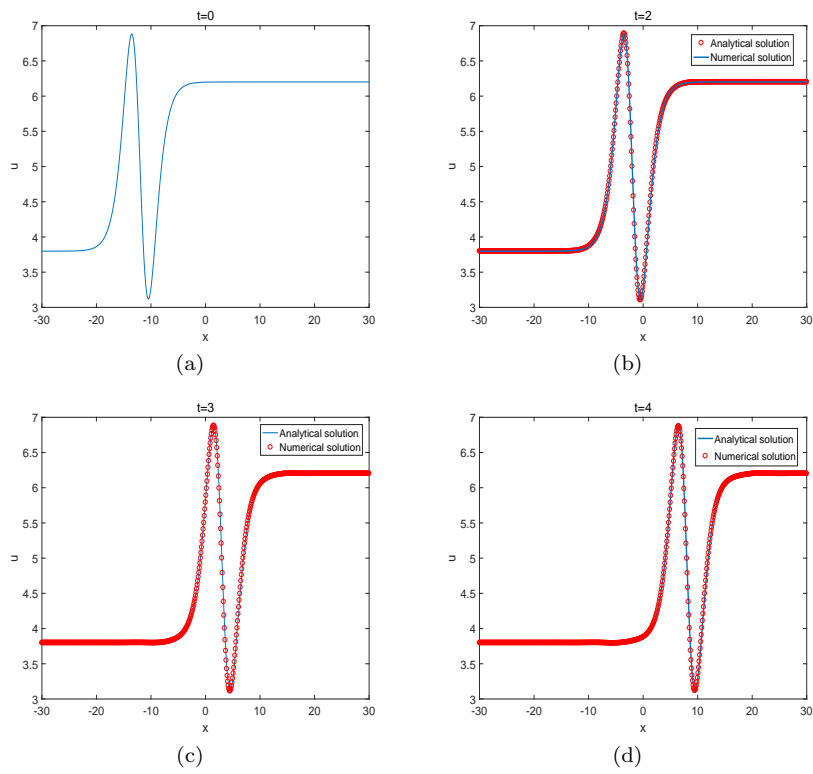


**Fig. 1** The shock profile wave propagation of the K-S equation.

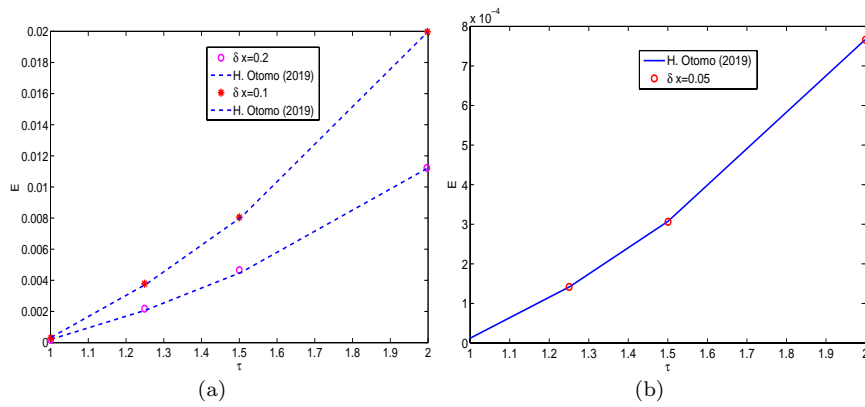


**Fig. 2** Global relative error  $E$  as a function of  $\tau$  with various lattice resolutions.

**Table 1**  $E$  with different lattice spacings,  $\delta t = 1.0 \times 10^{-4}$ .

$\delta x$	$E$ for model I	order	$E$ for model II	order
0.4	$2.0811 \times 10^{-2}$	–	$8.6820 \times 10^{-2}$	–
0.2	$5.3262 \times 10^{-3}$	1.9661	$2.3531 \times 10^{-2}$	1.8835
0.1	$1.3738 \times 10^{-3}$	1.9549	$6.3250 \times 10^{-3}$	1.8954
0.05	$3.5126 \times 10^{-4}$	1.9676	$1.7132 \times 10^{-3}$	1.8844

**Table 2**  $E$  with different time steps,  $\delta x = 0.001$ .

$\delta t$	$E$ for model I	order	$E$ for model II	order
$0.4 \times 10^{-3}$	$5.3153 \times 10^{-5}$	–	$8.8481 \times 10^{-5}$	–
$0.2 \times 10^{-3}$	$2.0182 \times 10^{-5}$	1.3971	$4.0283 \times 10^{-5}$	1.1352
$0.1 \times 10^{-3}$	$7.5098 \times 10^{-6}$	1.4262	$1.8126 \times 10^{-5}$	1.1521
$0.5 \times 10^{-4}$	$2.7846 \times 10^{-6}$	1.4313	$8.2163 \times 10^{-6}$	1.1415

## 4 Numerical results

### 4.1 LB model for Kuramoto-Sivashinsky equation

To verify the effectiveness of the proposed LBM, the following Kuramoto-Sivashinsky (K-S) equation with exact solutions are numerically solved

$$u_t + uu_x + u_{xx} + u_{xxxx} = 0. \quad (40)$$

The exact solution is

$$U(x, t) = b + \frac{15}{19} \sqrt{\frac{11}{19}} (-9 \tanh(k(x - bt - x_0)) + 11 \tanh^3(k(x - bt - x_0))), \quad (41)$$

In simulations, we set  $b = 5$ ,  $k = \frac{1}{2} \sqrt{\frac{11}{19}}$  and  $x_0 = -12$ . The simulation is conducted in  $[-30, 30]$  with  $\delta x = 0.1$ ,  $\delta t = 0.0001$  and  $\tau = 1.27$ .

The following global relative error is used to measure the accuracy:

$$E = \frac{\sum |u(\mathbf{x}, t) - U(\mathbf{x}, t)|}{\sum |U(\mathbf{x}, t)|}, \quad (42)$$

where  $u$  and  $U$  are the numerical solution and analytical one, respectively, and the summation is taken over all grid points. The regular shock profile wave propagation is presented in Fig. 1. It can be seen that the numerical results are agree well with those in reference [8].

It is worth mentioning that in the previous LB models, the fourth order NPDE is usually numerically solved as the second order convection diffusion equation. Such as the K-S equation, which is rewritten as  $u_t + uu_x + (u + u_{xx})_{xx} = 0$ . The last term  $(u + u_{xx})_{xx}$  is treated as diffusion term putting in the equilibrium distribution function in the previous LB model. For convenience, we call this LB model as model II, while the proposed model in this study is called as model I.

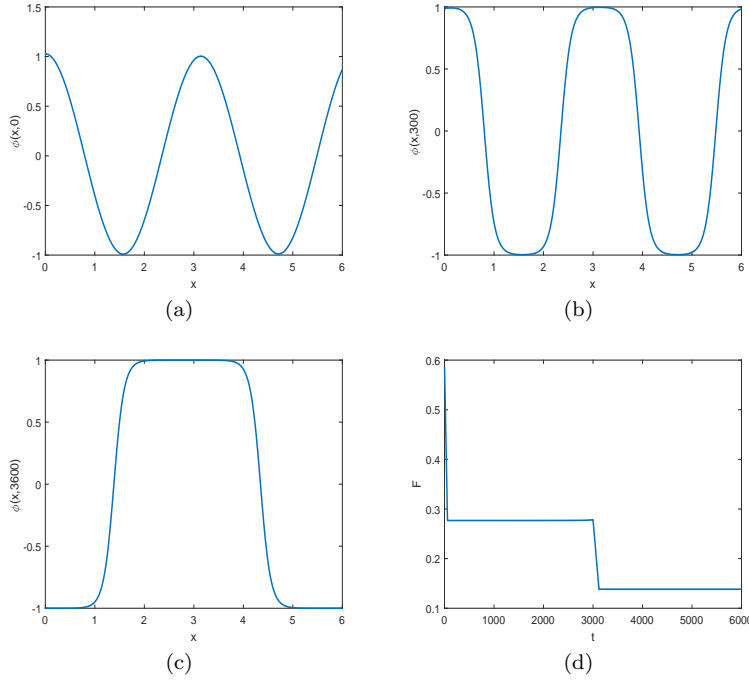


**Fig. 3** Numerical solution of the 1D Cahn-Hilliard equation: (a)  $t=0$ ; (b)  $t=300$ ; (c)  $t=3600$ ; (d) energy curve.

To compare the performance of these two models, error estimates with different lattice spacings and times steps are listed in Tables 1 and 2, respectively. It can be seen that both of these two models has second order accuracy in space. However, the time accuracy of model I is much better than model II.

Furthermore, to investigate the influence of relaxation time  $\tau$  on the truncation errors, the global relative error  $E$  as a function of  $\tau$  with various lattice resolutions are shown in Fig. 2. It can be observed that when  $\tau$  is away from one, the truncation error becomes large. It could be also observed that our results are consistent with those in [32].

#### 4.2 LB model for Cahn-Hilliard equation

We consider the 1D fourth order Cahn-Hilliard equation for a scalar function  $\phi(x, t)$ .

$$\phi_t = -\kappa\phi_{xxxx} + (f'(\phi))_{xx}, \quad (43)$$

where  $f(\phi) = \frac{1}{4}(\phi^2 - 1)^2$ . We consider  $x \in [0, 6]$  and  $\phi$  to be periodic in space. The initial data is set as

$$\phi_0(x) = \cos(2x) + \frac{1}{100} \exp^{\cos(x+1/10)}, \quad (44)$$

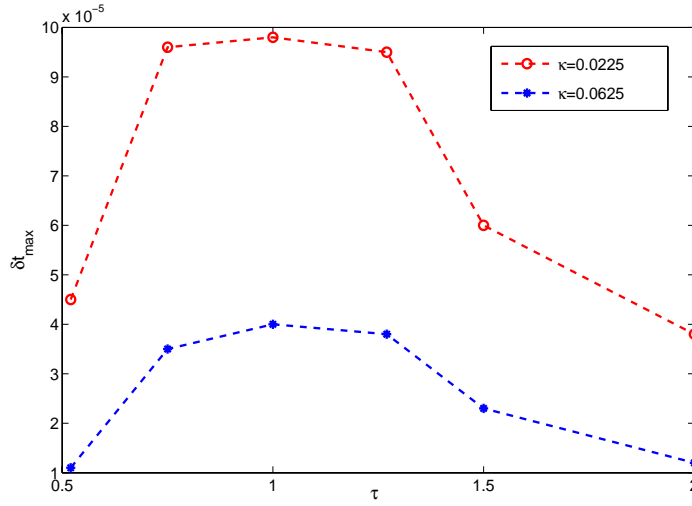


Fig. 4 The influence of  $\tau$  on the  $\delta t_{max}$ .

Table 3  $E_N$  with different lattice spacings,  $\delta t = 1.0 \times 10^{-6}$ ,  $\kappa = 0.0625$ .

$\delta x$	$E_N$ for model I	order	$E_N$ for model II	order
0.04	$9.322 \times 10^{-3}$	–	$1.562 \times 10^{-2}$	–
0.02	$2.396 \times 10^{-3}$	1.9642	$4.383 \times 10^{-3}$	1.8321
0.01	$6.244 \times 10^{-4}$	1.9382	$1.226 \times 10^{-3}$	1.8456
0.005	$1.593 \times 10^{-4}$	1.9659	$3.302 \times 10^{-4}$	1.8843

Table 4  $E_t$  with different time steps,  $\delta x = 0.02$ ,  $\kappa = 0.0625$ .

$\delta t$	$E_t$ for model I	order	$E_t$ for model II	order
$8.0 \times 10^{-7}$	$1.706 \times 10^{-4}$	–	$3.425 \times 10^{-4}$	–
$4.0 \times 10^{-7}$	$6.127 \times 10^{-5}$	1.4774	$1.649 \times 10^{-4}$	1.0544
$2.0 \times 10^{-7}$	$2.058 \times 10^{-5}$	1.5739	$7.881 \times 10^{-5}$	1.0653
$1.0 \times 10^{-7}$	$6.920 \times 10^{-6}$	1.5724	$3.978 \times 10^{-5}$	0.9865

Table 5  $\delta t_{max}$  with different  $\kappa$  and  $\delta x$ .

$\kappa$	$\delta x$	model I	model II
$0.15 \times 0.15$	0.04	$\delta t_{max} \approx 9.5 \times 10^{-5}$	$\delta t_{max} \approx 4.1 \times 10^{-5}$
	0.02	$\delta t_{max} \approx 6.6 \times 10^{-6}$	$\delta t_{max} \approx 2.6 \times 10^{-6}$
$0.25 \times 0.25$	0.04	$\delta t_{max} \approx 3.8 \times 10^{-5}$	$\delta t_{max} \approx 1.5 \times 10^{-5}$
	0.02	$\delta t_{max} \approx 2.4 \times 10^{-6}$	$\delta t_{max} \approx 9.6 \times 10^{-7}$

**Table 6** Relevant data of  $nC_4$ .

$T_c$ , K	$P_c$ , MPa	$T_b$ , K	a	b	$\kappa$	$n_g$	$n_l$
425.18	3.797	272.64	1.6944	$7.2442 \times 10^{-5}$	$2.0887 \times 10^{-3}$	403.17	8878.89

and  $\kappa = 0.0225$ . In simulations, we set the lattice spacing  $\delta x = 0.02$ , the time step  $\delta t = 6.0 \times 10^{-6}$  and  $\tau = 1.27$ . The numerical solutions of the above equation at different moments are presented in Fig. 3. It can be seen that the small perturbation in the right hand side of equation (44) makes the two intervals of the initial data not symmetric, so that the generic behaviour can be captured. As seen in Fig. 3 (b), the system moves to an intermediate state with two intervals at  $t = 300$ . Over a very long time, these two intervals evolve slowly and merge as shown in Fig. 3 (c). The evolution of the energy is present in Fig. 3 (d). It can be observed that the energy decreases after  $t = 3000$  so that we view the numerical solution in Fig. 3 (c) as the steady state. Next, in order to test the accuracy of the proposed LBM, error estimates  $E_N = \|\phi_N - \phi_{2N}\|$  and  $E_t = \|\phi_t - \phi_{t/2}\|$  with  $\kappa = 0.00625$  and  $\kappa = 0.0225$  to  $T = 0.5$  are presented in Tables 3 and 4, respectively. It is shown that the proposed LBM gives second-order accuracy in space, while the convergence order in time is about 1.5.

To further explore the performance of the proposed LBM, we define  $\delta t_{max}$  to be the largest possible time which allows stable numerical computation. If the time step is larger than its value, the numerical solution will blow up. As last subsection, we call the present LBM as model I for ease of comparison with other methods. While in previous studies [28,30,44,49,50], the CHE is numerically solved as the second order convection diffusion equation. In such way, the chemical potential  $\mu = (f'(\phi) - \kappa\phi_{xx})_{xx}$  is treated as a scalar putting in the equilibrium distribution function, we call this corresponding LB scheme as model II. The values of  $\delta t_{max}$ , which are computed by model I and model II with different  $\kappa$  and  $\delta x$ , are listed in Table 5. It can be seen that model I have better energy stability than model II, large time steps are allowed in the long time numerical simulations.

In addition, the choice of relaxation time  $\tau$  is very important to numerical stability of the present LBM. To investigate the influence of  $\tau$  on the numerical stability, the relationship between  $\tau$  and  $\delta t_{max}$  is depicted in Fig. 4. It can be seen that larger time steps can be used when the value of  $\tau$  is around one.

#### 4.3 LB model for the fourth-order diffuse interface model with Peng-Robinson equation of state

In this section, a fourth order diffuse interface model with Peng-Robinson (P-R) equation of state (EOS) is numerically studied by the present LB model. P-R EOS is the most popular equation of state used in oil reservoir simulation. The free energy of the P-R model is highly nonlinear and the molar densities of the two energy-lowest positions (which correspond to gas and liquid states) differ by orders of magnitudes, which are very difficult to be captured accurately, see [34] for detailed discussion. This model has been used to be a benchmark problem to test the reliability of developed numerical algorithms for phase-field problems, see e.g., [14,20,21,27,33].

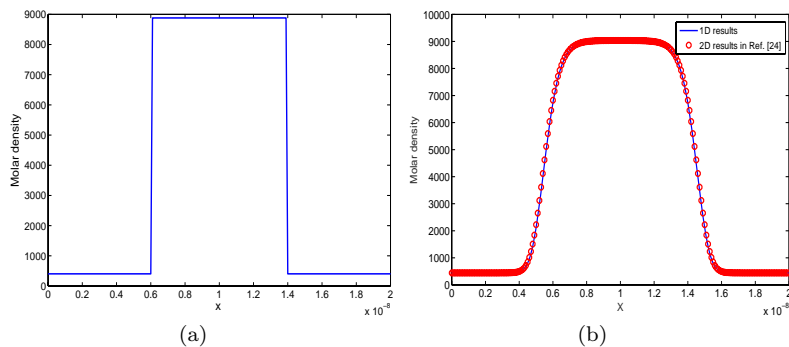


**Fig. 5** Numerical solution of the 1D single component two-phase diffuse interface model with P-R EOS: (a) initial data; (b) steady state.

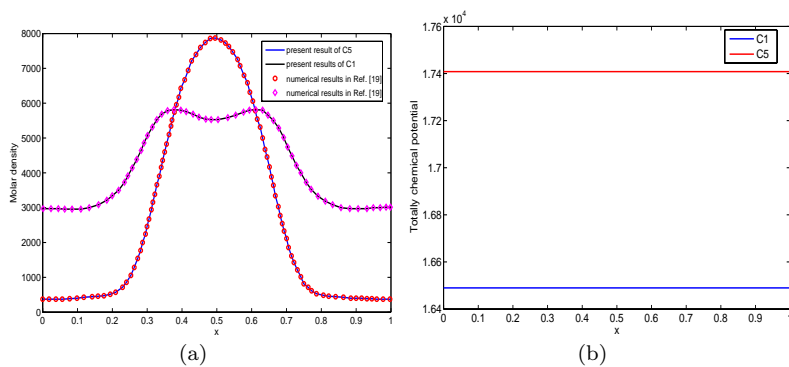


**Fig. 6** Numerical solution of binary mixture at 260K: (a) Molar density profiles; (b) Totally chemical potential profiles.

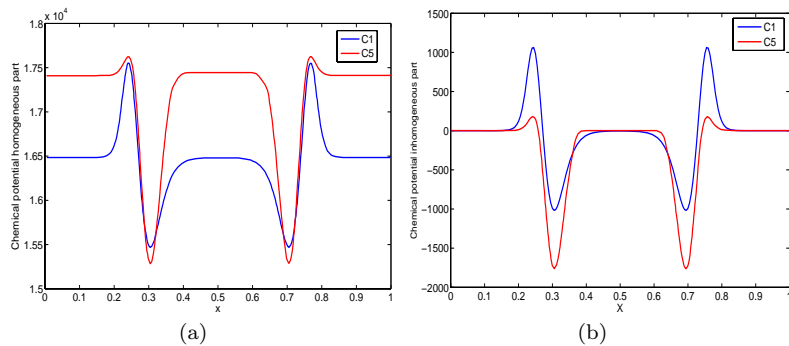


**Fig. 7** Numerical solution of binary mixture at 260K: (a) homogeneous chemical potential profiles; (b) inhomogeneous chemical potential profiles.

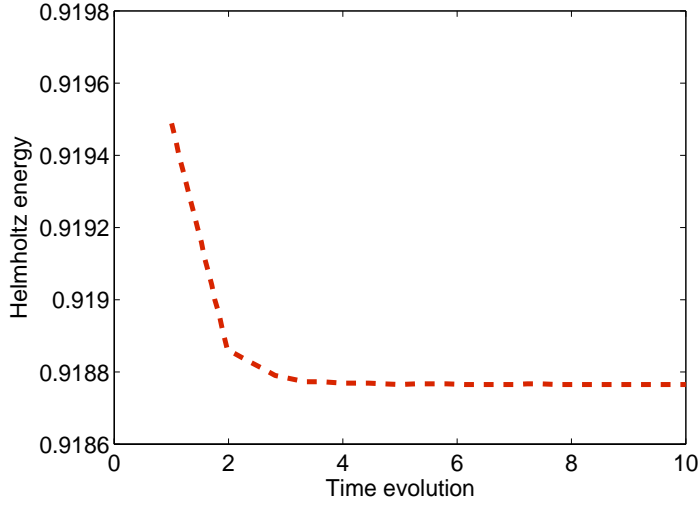


Fig. 8 Helmholtz energy with time evolution.

Considering a mixture composed of  $N$  ( $N \geq 2$ ) components and denoting the mixture composition by  $\mathbf{n} = [n_1, n_2, \dots, n_N]^T$ , where  $n_i$  is the molar density of the  $i$ th component, the multi-component fourth order diffuse interface model can be written as

$$\begin{aligned} \frac{\partial n_i}{\partial t} + \nabla \cdot \mathbf{J}_i &= 0, \\ \mathbf{J}_i &= -M_i \nabla \mu_i, \quad i = 1, \dots, N. \end{aligned} \quad (45)$$

Here  $\mathbf{J}_i$  is the flux of component  $i$ ,  $M_i > 0$  is the diffusivity, and  $\mu_i$  is the chemical potential of component  $i$ . Suppose that the influence parameter  $c_{ij}$  is independent of molar density, and then the chemical potential of the  $i$ -th component in an inhomogeneous fluid is calculated as

$$\mu_i = \mu_i^0(\mathbf{n}) - \sum_j c_{ij} \Delta n_j, \quad i = 1, \dots, N, \quad (46)$$

where  $\mu_i^0$  is the chemical potential of the  $i$ th component in a homogeneous fluid defined as

$$\mu_i^0 = \left( \frac{\partial f_0(\mathbf{n})}{\partial n_i} \right)_{T, n_1, \dots, n_{i-1}, n_{i+1}, \dots, n_N}. \quad (47)$$

Here,  $T$  represents the temperature, and  $f_0(\mathbf{n})$  is the Helmholtz free energy density of a homogeneous fluid. In this work, the realistic Peng-Robinson EOS, which is widely used in the oil industries and petroleum engineering, is considered. In this case,  $f_0(\mathbf{n})$  is expressed as summation of two terms, ideal part and excess one,

$$\begin{aligned} f_0(\mathbf{n}) &= f_0^{ideal}(\mathbf{n}) + f_0^{excess}(\mathbf{n}), \\ f_0^{ideal}(\mathbf{n}) &= RT \sum_{i=1}^M n_i (\ln n_i - 1), \\ f_0^{excess}(\mathbf{n}) &= -nRT \ln(1 - bn) + \frac{an}{2\sqrt{2}b} \ln \left( \frac{1 + (1 - \sqrt{2})bn}{1 + (1 + \sqrt{2})bn} \right), \end{aligned}$$

where  $R$  denotes the universal gas constant with the value of  $8.31432JK^{-1}mol^{-1}$ . The parameters  $a = a(T)$  and  $b$  are the energy parameter and the co-volume parameter, respectively. The definition of these two parameters can be found in Appendix.

In simulations, the Neumann-Neumann type boundary conditions are given by

$$\nabla n_i \cdot \nu_{\partial\Omega} = 0, \mathbf{J}_i \cdot \nu_{\partial\Omega} = 0, i = 1, \dots, N. \quad (48)$$

where  $\Omega \subset \mathbf{R}^d$  ( $1 \leq d \leq 3$ ) is an open, bounded and connected domain containing the two-phase fluid interface and  $\nu_{\partial\Omega}$  is the outward normal to the boundary  $\partial\Omega$ . The general bounce-back scheme in [48] is used to treat the macroscopic boundary conditions in the present work.

Next, we use the proposed LB model to simulate one-dimensional two-phase fluid interface problems. Firstly, the realistic hydrocarbon component isobutane ( $nC_4$ ) at temperature  $350K$  is simulated. The computational domain is  $\Omega = (0, L)$ , where  $L = 2 \times 10^{-8}$  meters. The critical properties, the initial molar densities of liquid  $n_l$  and gas  $n_g$ , and the normal boiling point of  $nC_4$  are provided in Table 6. The initial condition is set as Figure 5 (a). The whole discrete domain  $\Omega$  has 200 uniform grids and the time step is set as  $1.5 \times 10^{-7}$ . The numerical result at steady state is shown in Figure 5 (b). It can be seen that the one dimensional numerical result agree well with the two dimensional results in reference [35]. Moreover, the existing LB model (called model II) is also used to simulate this problem. It is found that the numerical solutions would not be of convergence by model II for any time steps.

Finally, the binary mixture, which is composed of methane ( $C_1$ ) and pentane ( $C_5$ ), is also studied by the proposed LB model. The Neumann-Neumann type boundary condition is considered. The binary interaction coefficients for the influence parameters are taken as  $\beta_{11} = \beta_{22} = 0$  and  $\beta_{12} = \beta_{21} = 0.5$ . The mobility  $M_i$  is taken to be a constant. We denote by  $\mathbf{n}^G = (n_1^G, \dots, n_N^G)$  and  $\mathbf{n}^L = (n_1^L, \dots, n_N^L)$  the molar density of the equilibrium bulk gas and liquid phases of a mixture, respectively. In the numerical tests, the temperature is kept at  $260$  K, one-dimensional domain  $(0, l_x)$  is taken, where  $l_x = 1.0 \times 10^{-8}m$ , and a uniform mesh with 100 elements is used. The time step is set as  $1.0 \times 10^{-7}$ . The initial condition of each component is to impose the  $C_1$  and  $C_5$  binary mixture with the composition  $0.8\mathbf{n}^L$  in the region of  $(0.3l_x, 0.7l_x)$ , and the rest of the domain is filled with the mixture composition  $0.8\mathbf{n}^G$ . The numerical results at steady state are depicted in Fig. 6, which have a well agreement with the previous work in reference [19]. In addition, to illustrate the thermodynamic consistent of the numerical results, the chemical potential of the binary mixture is shown in Fig. 6 (b) and Fig. 7. It can be seen that the chemical potential of each component is equal in every phase. Fig. 8 depicts the total Helmholtz free energy varying with time steps, where the energy decay is clearly observed.

#### 4.4 Conclusion

A novel LB equation model with an auxiliary source distribution function is proposed to solve the general fourth order NPDE. The effect of the source distribution function is to eliminate some unwanted terms in the nonlinear part of the fourth order NPDE. The C-E analysis shows that the general fourth order NPDE can be

recovered perfectly from the proposed LBM. Numerical tests demonstrated that the proposed LBM has second-order accuracy in space, and the convergence order in time is about 1.5. We make a comparison between the present LBM and previous existing models. The results have shown that the  $\delta t_{max}$  computed by the present LBM is much larger than the one by previous models. Furthermore, we make a simulation of a diffuse interface model with Peng-Robinson EOS which is difficult to be resolved by previous LB approaches. Our novel LBM is reliable to solve fourth-order NPDEs with nonlinear second-order terms, which could be very useful for the simulation of phase field problems. **In this work, we only consider 1D NPDEs on a D1Q5 lattice, where high order C-E and Taylor series expansions are used. However, it is technically difficult to apply the similar analysis directly to 2D or 3D LB models. A possible solution is to employ alternating direction methods in the analysis, which will be studied in the future work.**

### Acknowledgments

Z. Qiao's work is partially supported by Hong Kong Research Council GRF grant 15325816 and the Hong Kong Polytechnic University internal research fund G-UAey. X. Yang's work is partially supported by the Natural Science Foundation of China (Grant No. 11802090) and the Hong Kong Polytechnic University Post-doctoral Fellowships Scheme 1-YW1D.

### Appendix

The definition of parameters  $a(T)$  and  $b$  are given by the following mixing rules

$$a(T) = \sum_{i=1}^M \sum_{j=1}^M y_i y_j (a_i a_j)^{1/2} (1 - k_{ij}),$$

$$b = \sum_{i=1}^M y_i b_i,$$

where  $y_i = n_i/n$  is the mole fraction of component  $i$ ,  $k_{ij}$  is the binary interaction coefficient of Peng-Robinson EOS, which is usually computed from experimental correlation. The Peng-Robinson parameters  $a_i$  and  $b_i$  for pure-substance component  $i$  can be derived from the critical properties of the particular species as follows:

$$a_i(T) = 0.45724 \frac{R^2 T_{c_i}^2}{P_{c_i}} \left( 1 + m_i \left( 1 - \sqrt{\frac{T}{T_{c_i}}} \right) \right)^2, \quad b_i = 0.07780 \frac{R T_{c_i}}{P_{c_i}}.$$

Here,  $T_{c_i}$  and  $P_{c_i}$  represent the critical temperature and the critical pressure of a pure substance, respectively. The parameter  $m_i$  has the following relations with the acentric parameter  $\omega_i$ :

$$m_i = 0.37464 + 1.54226\omega_i - 0.26992\omega_i^2, \omega_i \leq 0.49,$$

$$m_i = 0.379642 + 1.485030\omega_i - 0.164423\omega_i^2 + 0.016666\omega_i^3, \omega_i > 0.49.$$

The acentric parameter  $\omega_i$  can be computed by using critical temperature  $T_{c_i}$ , critical pressure  $P_{c_i}$  and the normal boiling point  $T_{b_i}$ :

$$\omega_i = \frac{3}{7} \left( \frac{\log_{10} \left( \frac{P_{c_i}}{14.695 \text{ PSI}} \right)}{\frac{T_{c_i}}{T_{b_i}} - 1} \right) - 1.$$

The cross influence parameter  $c_{ij}$  can be obtained by using the modified geometric mean rule

$$c_{ij} = (1 - \beta_{ij}) \sqrt{c_i c_j},$$

where  $\beta_{ij}$  represents the binary interaction coefficient for the influence parameter. Its value is usually assumed to be zero in most engineering practice.  $c_i$  is the pure component influence parameter, which is related to the Peng-Robinson parameters  $a_i$  and  $b_i$  by [3]

$$c_i = a_i b_i^{2/3} \left( m_{1,i}^c \left( 1 - \frac{T}{T_{c_i}} \right) + m_{2,i}^c \right),$$

here,  $m_{1,i}^c$  and  $m_{2,i}^c$  denote the coefficients which can be related to the acentric factor  $\omega_i$  by

$$m_{1,i}^c = -\frac{10^{-16}}{1.2326 + 1.3757\omega_i}, m_{2,i}^c = \frac{10^{-16}}{0.9051 + 1.5410\omega_i}.$$

## References

1. Allen S. M., Cahn J. W.: Mechanisms of phase transformations within the miscibility gap of Fe-rich Fe-Al alloys. *Acta Metall.* 24, 425-437 (1976).
2. Anderson D. M., McFadden G. B., Wheeler A. A.: Diffuse-interface methods in fluid mechanics. *Annu. Rev. Fluid Mech.* 30, 139-165 (1998).
3. Breure B., Peters C. J.: Modeling of the surface tension of pure components and mixtures using the density gradient theory combined with a theoretically derived influence parameter correlation, *Fluid Phase Equil.*, 334, 189-196 (2012).
4. Cahn J. W., Hilliard J. E.: Free energy of a non-uniform system free energy. *J. Chem. Phys.* 28, 258-267 (1958).
5. Chiu P.H., Lin Y. T.: A conservative phase field method for solving incompressible two-phase flows. *J. Comput. Phys.* 230, 185-204 (2011).
6. Aidun C., Clausen J.: Lattice Boltzmann method for complex flows. *Annu. Rev. Fluid Mech.* 42, 439-372 (2010).
7. Chai Z. H., Shi B. C., Guo Z. L.: A Multiple-Relaxation-Time Lattice Boltzmann Model for General Nonlinear Anisotropic Convection-Diffusion Equations. *J. Sci. Comput* 69, 355-390 (2016).
8. Chai Z. H., He N. Z., Guo Z. L., Shi B. C.: Lattice Boltzmann model for high-order nonlinear partial differential equations. *Phy. Rev. E* 97, 013304 (2018).
9. Chai Z., Shi B., Zheng L.: A unified lattice Boltzmann model for some nonlinear partial differential equations. *Chaos Solitons Fractals* 36, 874-882 (2008).
10. Chen L., Kang Q., Tang Q. et al: Pore-scale simulation of multicomponent multiphase reactive transport with dissolution and precipitation. *Int. J Heat Mass Tran.* 85, 935-949 (2015).
11. Chen L. J., Ma C. F.: A lattice Boltzmann model with an amending function for simulating nonlinear partial differential equations. *Chin. Phys. B* 19, 010504 (2010).
12. Chen S., Doolen G.: Lattice Boltzmann method for fluid flows. *Annu. Rev. Fluid Mech.* 30, 329-364 (1998).
13. Gunstensen A. K., Rothman D. H., Zaleski S., Zanetti G.: Lattice Boltzmann model of immiscible fluids. *Phys. Rev. A* 43, 4320-4327 (1991).

14. Fan X., Kou J., Qiao Z., Sun S.: A componentwise convex splitting scheme for diffuse interface models with van der Waals and Peng-Robinson equations of state. *SIAM Journal on Scientific Computing*, 39, B1–B28, (2017).
15. Geier M., Fakhari A., Lee T.: Conservative phase-field lattice Boltzmann model for interface tracking equation. *Phys. Rev. E* 91, 063309 (2015).
16. Guo Z., Shu C.: *Lattice Boltzmann method and its applications in engineering*. World Scientific Publishing, Singapore, 2013.
17. Guo Z., Zheng C., Zhao T.: A lattice BGK scheme with general propagation. *J. Sci. Comp.* 16(4): 569-585 (2001).
18. Kim J.: Phase-field models for multi-component fluid flows. *Commun. Comput. Phys.* 12, 613-661 (2012).
19. Kou J., Sun S.: Unconditionally stable methods for simulating multi-component two-phase interface models with Peng-Robinson equation of state and various boundary conditions. *J. Comput. Appl. Math.* 291, 158-182 (2016).
20. Kou J., Sun S., Wang X.: Linearly decoupled energy-stable numerical methods for multi-component two-phase compressible flow. *SIAM Journal on Numerical Analysis*, 56, 3219-3248, (2018).
21. Kou J., Sun S., Wang X.: A novel energy factorization approach for the diffuse-interface model with Peng-Robinson equation of state. *SIAM J. Sci. Comput.* 42, B30-B56, (2020).
22. Ladd A.: Numerical simulations of particle suspensions via a discretized Boltzmann equation. Part 2. Numerical results. *J. Fluids Mech.* 271, 311 (1994).
23. Ladd A., Verberg R.: Lattice-Boltzmann simulations of particle-Fluid suspensions. *J. Stat. Phys.* 104, 1191-1251 (2001).
24. Lai H., Ma C.: Lattice Boltzmann method for the generalized Kuramoto-Sivashinsky equation. *Phys. A (Amsterdam)* 388, 1405-1412 (2009).
25. Lai H., Ma C.: The lattice Boltzmann model for the second-order Benjamin-Ono equations. *J. Stat. Mech.* 2010, P04011 (2010).
26. Lee T., Lin C. L.: A stable discretization of the lattice Boltzmann equation for simulation of incompressible two-phase flows at high density ratio. *J. Comput. Phys.* 206, 16-47 (2005).
27. Li H., Ju L., Zhang C., Peng Q.: Unconditionally energy stable linear schemes for the diffuse interface model with Peng-Robinson equation of state. *Journal of Scientific Computing*, 75, 993–1015, (2018).
28. Li Q., Luo K. H., Gao Y. J., He Y. L.: Additional interfacial force in lattice Boltzmann models for incompressible multiphase flows. *Phys. Rev. E*, 85, 026704 (2012).
29. Li Q., Luo K., Kang Q., He Y., et al.: Lattice Boltzmann methods for multiphase flow and phasechange heat transfer. *Prog. Energ. Combust.* 52, 62-105 (2016).
30. Liang H., Shi B., Guo Z. L., Chai Z. H.: Phase-field-based multiple-relaxation-time lattice Boltzmann model for incompressible multiphase flows. *Phys. Rev. E* 89, 053320 (2014).
31. Liu H., Kang Q., Leonardi C. R., et al.: Multiphase lattice Boltzmann simulations for porous media applications. *Computational Geosciences* 20, 777-805 (2014).
32. Otomo H.: *Lattice Boltzmann Models for Higher-Order Partial Differential Equations*, Ph.D. Thesis, Tufts University, 2019.
33. Peng Q.: A convex-splitting scheme for a diffuse interface model with Peng-Robinson equation of state. *Advances in Applied Mathematics and Mechanics*, 9, 1162–1188, (2017).
34. Qiao Z., Sun S.: Two-phase fluid simulation using a diffuse interface model with Peng-Robinson equation of state. *SIAM Journal on Scientific Computing*, 36, B708–B728, (2014).
35. Qiao Z., Yang X., Zhang Y.: Mass conservative lattice Boltzmann scheme for a three-dimensional diffuse interface model with Peng-Robinson equation of state. *Phys. Rev. E*, 98(2): 023306, 2018.
36. Shan X., Chen H.: Lattice Boltzmann model for simulating flows with multiple phases and components. *Phys. Rev. E* 47, 1815-1819 (1993).
37. Shen J., Yang X.: A phase-field model and its numerical approximation for two-phase incompressible flows with different densities and viscosities. *SIAM J. Sci. Comput.* 32, 1159V1179 (2010).
38. Shi B., Guo Z.: Lattice Boltzmann model for nonlinear convection-diffusion equations. *Phys. Rev. E* 79, 016701 (2009).
39. Succi, S.: A note on the lattice Boltzmann versus finite-difference methods for the numerical solution of the Fishers equation. *Int. J. Mod. Phys. C* 25, 1340015 (2014).
40. Wang Y., Shu C., Huang H. B., Teo C. J.: Multiphase lattice Boltzmann flux solver for incompressible multiphase flows with large density ratio. *J. Comput. Phys.* 280, 404-423 (2015).

41. Wang Y., Shu C., Shao J. Y., Wu J., Niu X. D.: A mass-conserved diffuse interface method and its application for incompressible multiphase flows with large density ratio. *J. Comput. Phys.* 290, 336-351 (2015).
42. Yan G., Zhang J.: A higher-order moment method of the lattice Boltzmann model for the Korteweg-de Vries equation. *Math. Comput. Simulat.* 79, 1554-1565 (2009).
43. Yan G. W.: A lattice Boltzmann equation for waves. *J. Comput. Phys.* 161, 61-69 (2000).
44. Yang K., Guo Z.: Lattice Boltzmann method for binary fluids based on mass-conserving quasi-incompressible phase-field theory. *Phys. Rev. E* 93, 043303 (2016).
45. Ye L., Yan G., Li T.: Numerical method based on the lattice Boltzmann model for the Kuramoto-Sivashinsky equation. *J. Sci. Comput.* 49, 195-210 (2011).
46. Yu, X. M., Shi, B. C.: A lattice BhatnagarVGGrossVKrook model for a class of the generalized Burgers equations. *Chin. Phys.* 15, 1441V1449 (2006).
47. Zhang Z., Qiao Z.: An adaptive time-stepping strategy for the Cahn-Hilliard equation. *Commun. Comput. Phys.* 11, 1261V1278 (2012).
48. Zhang T., Shi B.C., Guo Z.L., et al.: General bounce-back scheme for concentration boundary condition in the lattice Boltzmann method. *Phys. Rev. E* 85 (2012) 016701.
49. Zheng L., Zheng S., Zhai Q.: Lattice Boltzmann equation method for the Cahn-Hilliard equation. *Phys. Rev. E* 91, 013309 (2015).
50. Zu Y. Q., He S.: Phase-field-based lattice Boltzmann model for incompressible binary fluid systems with density and viscosity contrasts. *Phys. Rev. E* 87, 043301 (2013).